

# Flexural Stiffness of Normal and Sandwich Reinforced Concrete Beam Exposed to Fire Under Fixed Loading

*by Suryawan Murtiadi*

---

**Submission date:** 04-Mar-2023 05:03PM (UTC-0600)

**Submission ID:** 2028894100

**File name:** B1-5\_journal.pdf (563.69K)

**Word count:** 6224

**Character count:** 29888

# Flexural Stiffness of Normal and Sandwich Reinforced Concrete Beam Exposed to Fire Under Fixed Loading

A. Akmaluddin, S. Murtiadi, B. Anshari

**Abstract** – This study focuses on the experimental investigation of normal and sandwich reinforced concrete beam exposed to fire in order to evaluate their flexural stiffness. Two beams specimen of 200×300×4000 mm have been cast and tested under flexural loading. The first one has been a normal concrete beam (N) and the second one has been a sandwich concrete beam (SW) with 50 mm skin thickness and 200 mm core thickness. The skin compressive strength of 25 MPa and the core compressive strength of 15 MPa have been considered. The skin strength has been also applied to the N beam. The beams have been reinforced with a plain bar of 3φ12 as a tensile reinforcement and 2φ10 as compression reinforcement. Both the tensile and the compression reinforcement have yield strength of 300 MPa. The beams have been tested in a full-size furnace under standard fire testing. Nine thermocouples for measuring temperature have been mounted. An LVDT, which has been protected by fire-resistant material, has been placed at the center of the beam to measure the deflection. The 8.63 kN load has been employed at 1/3 span of the beam. Test results have showed that the flexural stiffness of the beam strongly affected by the accumulative temperature representing temperature and firing time. The strength of the N beam drops significantly after 15 minutes of firing and the beam strength has been totally lost. The firing of 45 minutes has needed to decrease the strength of the SW beam then has decreased gradually until 120 minutes of firing. Copyright © 2020 Praise Worthy Prize - All rights reserved.

**Keywords:** Beam, Sandwich, Concrete, Fire, Flexural Stiffness

## Nomenclature

$A_s$	Area of tensile reinforcement [mm <sup>2</sup> ]
$a$	Shear span of beam [mm]
$a_c$	Height of equivalent stress block [mm]
$b$	Width of beam [mm]
$c$	Height of stress block [mm]
$d$	Effective depth of beam [mm]
$D$	Beam deflection limit under fire [mm]
$E_c$	Concrete modulus of elasticity [MPa]
$E_s$	Steel modulus of elasticity [MPa]
$f'_c$	Concrete compressive strength [MPa]
$f_r$	Modulus of rupture, $0.75 \times 0.62 \sqrt{f'_c}$
$f_y$	Yield strength of steel [MPa]
$h$	Height of beam [mm]
$h_s$	Skin thickness of sandwich beam [mm]
$I_{cr}$	Cracking moment of inertia [mm <sup>4</sup> ]
$I_e$	Effective moment of inertia [mm <sup>4</sup> ]
$I_g$	Gross moment of inertia ignoring steel [mm <sup>4</sup> ]
$L$	Span [m]
$M$	Moment [kNm]
$n$	Modular ratio of normal concrete to tensile steel
$n'$	Modular ratio of lightweight concrete to tensile steel
$P$	Total point load [kN]

$t$	Time limit of fire [minute]
$\delta$	Deflection [mm]
$\delta_{exp}$	Experimental deflection [mm]
$\rho$	Tensile reinforcement ratio

## I. Introduction

Fire is a disaster that can take lives and damage the infrastructure. It can also be described as one of the most severe environmental conditions in which concrete structure may be imposed [1]-[23]. The behavior of the reinforced concrete beams under fires has been studied through both numerical and experimental studies [1]-[4].

The effect of fires on reinforced concrete structures can cause strength degradation of concrete and decreasing beam stiffness as reported by several researchers [3], [5]-[7]. Recently, high temperatures (in hot climates) have attracted researchers to study this phenomenon on concrete performance and the results have showed that high temperatures have greatly reduced concrete performance [8]. On the other hand, additional cement material and coal waste have been more effective in increasing concrete properties [9], [10]. Repairing the damaged structure has also been a concern of the researchers by strengthening the structure with several techniques and materials. Then, the strengthening structures are further studied in terms of when the structure experiences a fire. The beams strengthened with

carbon fiber material have become a popular topic to study in order to see how much influence the fire has on the strengthening whether with or without the additional layer of fire retardant as studied by numerous researcher [11]-[13]. The study of concrete structures considering the effect of an explosion has also been studied recently. This is inspired since most of the structural materials applied in the city are flammable so it will cause an explosion when firing occurs [14]. Reinforced sandwich concrete beams made with different quality concrete layers have been studied under ideal conditions producing a model in order to estimate the sandwich beam stiffness [15]. This sandwich system has showed good behavior under testing at the ideal condition and it has the potential to be applied as a structural element for building construction, so it needs to be studied further when these elements are exposed to fire. Therefore, this study is intended to contribute to enriching knowledge about the behavior, resilience, and weaknesses of the reinforced sandwich concrete beams at elevated temperature. The number of studies is limited in the literature discussing the flexural stiffness of reinforced concrete-sandwich beams loaded and exposed to fire. The sandwich system adopted in this study has many benefits including high rigidity and low weight ratio [16] with the use of pumice as a lightweight concrete core in the sandwich system. This is intended to reduce beam self-weight since the pumice has lower density and acceptable performance [17], [18]. This study purpose is to investigate the flexural stiffness of sandwich beams through the behavior of normal and sandwich reinforced concrete beam under a fixed loading exposed to fire. In order to achieve the objective of this study, the sandwich concrete beam and the normal concrete beam with the same amount of reinforcement and configuration have been prepared and tested. Furthermore, the results obtained from this test which include the behavior of reinforced normal concrete beams and a reinforced sandwich concrete beam will be discussed and compared with each other.

## II. Failure Criteria

Failure criteria in the testing of a beam specimen under fire have often referred to failure time which is defined as the time consumed to release the entire bottom of the beam insulation, where the temperature increase of the concrete surface of the beam exceeds 50 K/min [11].

Indonesia Standard [19] accommodate the beam failure criteria during fire testing, which is interpreted as a time to reach the deflection limit,  $D$ , given as Eq. (1) or limiting the rate of deflection  $dD/dt$ , expressed as Eq. (2):

$$D = \frac{L^2}{400 d} \quad (1)$$

$$\frac{dD}{dt} = \frac{L^2}{9000 d} \quad (2)$$

In anticipating the high-risk tendency of the collapsing beam into the furnace space, then the test will be ceased when only one of the criteria mentioned above is exceeded. This approach is permitted by Standard [19] which is usually used to assess the fire resistance of beams. In practice, with respect to these beam specimens, the time difference in exceeding both criteria can be ignored.

## III. Loading Estimation

In order to estimate the magnitude of the specified load setup in this study, the section analysis of the sandwich beam has been carried out. The load has been generated from the maximum moment capacity of the section obtained using Eq. (3) below:

$$M = A_s f_y \left( d - \frac{a_c}{2} \right) \quad (3)$$

The depth of stress block  $a_c$  in the equation can be obtained using Eq. (4) when the neutral axis lies within the skin layer of the beam, otherwise,  $a_c$  in the equation should be replaced by  $h_s$  as demonstrated in [15]:

$$a_c = \frac{A_s f_y}{0.85 f_c'} \quad (4)$$

Once the value of  $M$  has been obtained, the total load  $P$ , which is distributed to two-point load at  $1/3$  span, can be estimated from the relation of the simple beam calculations as shown in Eq. (5) below:

$$P = \frac{6M}{L} \quad (5)$$

## IV. Deflection

The beams deflection subjected to two symmetrical points load can be calculated using Eq. (6) below:

$$\delta = \frac{M}{48EI} (3L^2 - 4a^2) \quad (6)$$

Modulus of elasticity,  $E$ , in the equation represents the concrete modulus of elasticity generated from the concrete compressive strength relationship as shown by Eq. (7) for normal concrete. If this is applied to lightweight concrete, then Eq. (7) should be multiplied by 0.75:

$$E_c = 4700 \sqrt{f_c'} \quad (7)$$

Moment of inertia,  $I$ , for both beam types is used as in [15], [20]. Since the beams are composed of brittle

materials where cracks are easy to perform when tensile stress occurs, then the moment of inertia value has taken into account the presence of cracking which is known as the effective moment of inertia,  $I_e$ , as Eq. (8). This equation is valid for  $M/M_{cr} > 1$ , otherwise  $I_e = I_g$ :

$$I_e = I_{cr} + \left( I_g - I_{cr} \right) \left( \frac{M_{cr}}{M} \right)^3 \quad (8)$$

where  $M_{cr}$  is calculated using Eq. (9) below.  $I_g$  and  $I_{cr}$  for sandwich concrete has been adopted as in [15] and rewritten for convenience as Eq. (10) and Eq. (11) respectively. In terms of the normal concrete beam, this equation can be applied by replacing  $n'$  equal to zero in the equation as demonstrated previously by the author in [15]:

$$M_{cr} = \frac{f_r I_g}{y_t} \quad (9)$$

$$I_g = \frac{1}{12} b h^3 + \frac{n'-1}{6} b h_s^3 + \frac{n'-1}{2} b h_s (h-h_s)^2 \quad (10)$$

$$I_{cr} = \frac{b c^3}{3} + \frac{(n'-1)}{12} b h_s^3 + (n'-1) b h_s \left( c - \frac{h_s}{2} \right)^2 + n A_s (d - c)^2 \quad (11)$$

The value of  $c$  in Eq. (11) can be generated from Eq. (12):

$$c = k d \quad (12)$$

where  $k$  is a general solution of the ABC quadratic equation as Eq. (13):

$$k = \frac{-B + \sqrt{B^2 - 4AC}}{2A} \quad (13)$$

where  $A = 1 + 2(n'-1)h_s$ ,  $B = -2 \left( (n'-1) \frac{h_s^2}{d} - n\rho \right)$  and

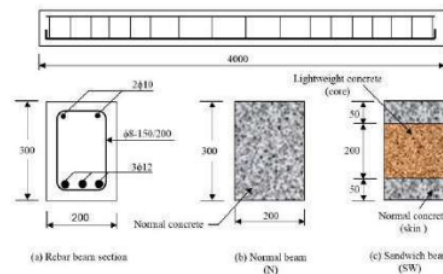
$$C = \left( (n'-1) \frac{h_s^2}{2d^2} - 2n\rho \right).$$

## V. Experimental Program

### V.1. Specimens Details

Two beams of 200x300x4000 mm have been made of normal concrete and sandwiches concrete (the combination of normal and lightweight concrete) as shown in Fig. 1(b) and Fig. 1(c) respectively. Fig. 1(a) shows three plain bars of 12 mm since tensile

reinforcement has been installed at the bottom of the beams. Compression reinforcements have been performed using two plain bars of 10 mm diameter placed at the top of the beams. Both reinforcements have a yield strength of 300 MPa. The beam made of normal concrete (N) as shown in Fig. 1(b) has a compressive strength of 25 MPa. The beam composed of normal and lightweight concrete as shown in Fig. 1(c) is denoted as SW, in which the compressive strength of 25 and 15 MPa respectively. In order to obtain temperature information during the beams testing in the furnace test rig, a number of thermocouples have been installed. The thermocouples have been attached at the bottom and the top of the concrete beam surface and also at the tensile reinforcement embedded in the beam. The latter has been intended to obtain the effect of concrete cover in protecting the reinforcement. The details arrangement of the thermocouples installed has been denoted as  $T_1, T_2, T_3 \dots, T_9$  as shown in Fig. 2. The beams considered in this study have been cast following the mixed compositions listed in Table I. Once the beams cast have been finished, the beams have been allowed drying out at the outside air temperature for a day. After that, the beams have been released from the mold, covered with wet burlap, and watered in order to keep it moist until 28 days. Then, the beams have been allowed to dry naturally until 90 days the age of testing. The cylinder specimens of 150 mm diameter and height of 300 mm have been cast in which the concrete has been taken from each batch of the beam concrete mix. The cylinders have been tested at the age of 28 days and at the same age as the beam test.



Figs. 1. Sketch of beam specimen

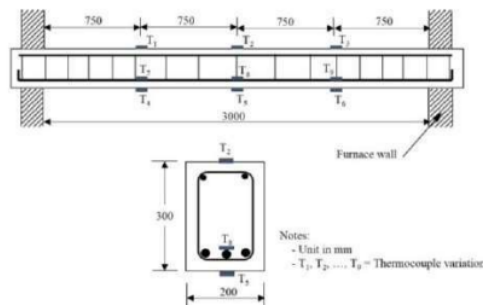


Fig. 2. Detail of thermocouples installed in the beam

TABLE I  
CONCRETE MIX PROPORTION FOR 1 m<sup>3</sup> VOLUME

No.	Ingredients	Lightweight concrete (LC)	Normal concrete (NC)
1	Cement (kg)	406	342
2	Water (kg)	203	205
3	Pumice (kg)	458	-
4	Sand (kg)	560	747
5	Gravel (kg)	-	1121

V.2. Specimen Properties

The target strengths of normal concrete and lightweight concrete considered in this study have been 25 and 15 MPa respectively. The Ordinary Portland Cement (OPC) with the trademark of "Semen Gresik" has been used in this study. The fine aggregate of sand and the coarse aggregate with a maximum size of 5 mm and 20 mm have been used respectively.

The fineness modulus of 2.56 and 6.98 has been obtained from preliminary testing of sand and gravel respectively. The mixtures proportion of normal concrete and lightweight concrete for 1 m<sup>3</sup> concrete volume are presented in Table I.

V.3. Test Set-Up and Instrumentation

The beam has been initially given a fixed load created from 1070 mm by 1050 mm and 160 mm thickness of the concrete slab. This slab has a weight  $\{2 \times (1.07 \text{ m} \times 1.05 \text{ m} \times 0.16 \text{ m} \times 24 \text{ kN/m}^3)\} = 8.63 \text{ kN}$ . The maximum capacity of the beam obtained from Eq. (5) has been 27.58 kN. Therefore, the fixed load determined in this study has been about 32.29% of the collapse load. The thermocouples installed as described in the previous section have been connected to the data logger to record temperatures. An LVDT has been attached in the middle of the beam to measure the deflection. The deflection has been read every 15 minutes, started from 0 to 120 minutes. The maximum firing time set has been 120 minutes. The test temperature has been controlled under the standard fire curve of SNI 1741: 2008 [19].

On the day of the testing time, the load has been attached permanently on the beam specimen prior to the erection on the testing furnace as can be seen in Fig. 3.

Once the beam has been ready to be tested, the fire has been turned on through the available control machines.



Fig. 3. Beam specimen fire test set-up

VI. Experimental Results and Discussions

VI.1. Concrete Quality

Concrete quality is expressed as concrete compressive strength obtained from testing of the cylindrical specimens at the age of 28 days. In this study, the cylindrical concrete specimens have been tested at 28 days and 91 days as explained previously. Testing at the age of 91 days has been intended to meet the same age as the beam test. The results obtained are presented in Table II. The table clearly shows that there is a significant improvement in terms of the compressive strength from the standard compressive strength (at 28 days) to the compressive strength on the day of testing (91 days), especially for the lightweight concrete which is about over 30% while for normal concrete the compressive strength increased by 20%. Then, the concrete compressive strength at the age of 91 days has been considered in the analysis and discussion in this chapter.

The test results clarify that the desired target strength criteria before testing the beam under fire have been met.

Structure behavior of the beam with fixed loading and exposed to fire is investigated through the relationship of firing time against temperature as presented in Fig. 4 and Fig. 5 for the normal beam (N) and sandwich beam (SW) respectively. It can be seen from the figures that the temperature on the surface of the concrete beam during the firing time for both beams are not significantly different. At the first 5 minutes of firing time, the concrete beam surface temperature has been above 500 °C. The longer the firing time is, the higher the temperature is. The reinforcement temperature also increases with firing time, the maximum rebar temperature is reached at 120 minutes of firing time of 474 and 447 °C for N and SW as shown in Fig. 4 and Fig. 5 respectively.

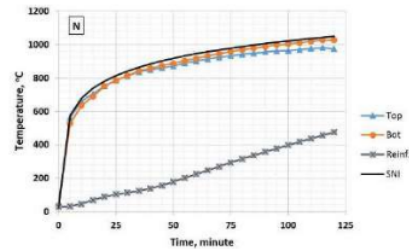


Fig. 4. The normal beam behavior under fire

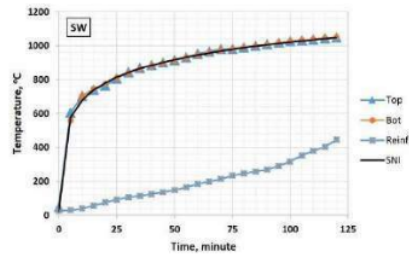


Fig. 5. The sandwich beam behavior under fire

TABLE II  
THE CONCRETE COMPRESSIVE STRENGTH OF CYLINDERS SPECIMEN

Type	Compressive Strength (MPa)		Improvement (%)	
	28 days	average	91 days	average
Lightweight concrete	11.0	11.1	15.20	31.76
	10.6	7	14.10	
	11.9		19.84	
	25.8		26.00	
Normal concrete	17.5	20.3	25.50	20.11
	7	22.30		
	17.8	28.20		

The increasing temperatures of the beam surface are not extreme as it has been of 500 °C in the first 5 minutes. The increasing temperature has decreased drastically from 100 °C to 5 °C. Typically, the temperature changing trend is decreased following a power function as shown inside Fig. 6. The increasing temperatures of reinforcement embedded in the beam are fluctuating as demonstrated by Fig. 7. In the figure, it is clearly shown that within the range of 0 to 15 minutes the temperature changing is increased then it decreases within the range of 15 to 35 minutes. After that, the changing trend of temperature is increased then it remains stable at about 20 °C. In general, the reinforcement embedded in concrete experience lowers temperatures during fire testing as presented in Fig. 4 and Fig. 5.

The temperature is lower than the maximum temperature allowed by 593 °C as stated in [21]. This concludes that concrete can effectively protect the steel reinforcement embedded in concrete. Thus, the SW has protected the steel reinforcement better than the N.

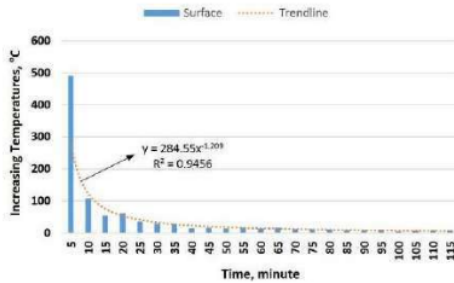


Fig. 6. The typical increasing temperature on the beam surface

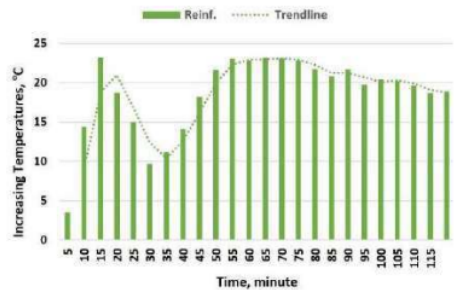


Fig. 7. Typical increasing temperature in the embedded reinforcement

### VI.2. Time-Deflection Relationship

The test specimen has been loaded with a fixed load of 8.63 kN. The load has been simplified working as two points loads acting at the 1/3 span of the beam. The variable observed is the value of deflection that occurs during the firing time process. Fig. 8 shows the behavior of N under elevated temperature. At the beginning of firing time, the first 15 minutes, the deflection value has increased significantly from zero to 5 mm (in negative sign). Then, the deflection goes gradually with its incremental value of less than 0.5 mm. Until the firing time limit of 120 minutes, the N shows a deflection of 8.8 mm (in negative sign). For the SW shown in Fig. 9, the deflection value is much smaller than the one of N (Fig. 8). The deflection of the SW in the first 15 minutes of firing time is 0.2 mm, and then it is relatively stable until the firing time of 45 minutes. From the 50th minute to the 90th minute of firing time, the deflection increases by about 0.1 to 0.2 mm. Finally, after the firing time of 90 minutes, the deflection has increased significantly with the value of 1.7 and 3.2 mm (in negative sign) for a firing time of 105 minutes and 120 minutes respectively.

When comparing the two types of beams above, it can be concluded that the SW is stiffer than the N when both are subjected to fire. This is certainly one of the advantageous of the SW application. Based on the stability requirements according to the SNI stated in the Eq. (1) then these two beams are still in the stable category because the deflection limit of  $L^2/(400d) = 92.21$  mm has not been exceeded. Stability limits according to the Eq. (2) is not applied due to the deflection that occurs in both beams that are still smaller than  $L/30$  or equal to 100 mm.

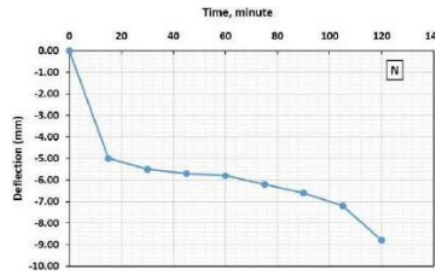


Fig. 8. Deflection and firing time of N

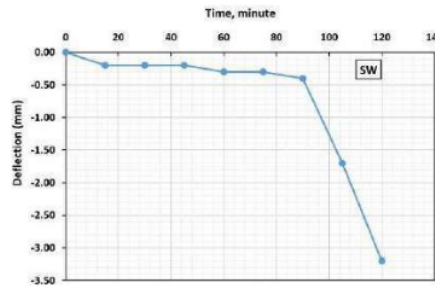


Fig. 9. Deflection and firing time of SW

VI.3. Flexural Stiffness

Referring to Eq. (13), flexural stiffness experimentally can be calculated using the following equation:

$$EI = \frac{1}{\delta_{exp}} \frac{M}{48} (3L^2 - 4a^2) \tag{14}$$

Eq. (14) above can be simplified as Eq. (15) due to some parameters have fixed values, such as load and its positions, span, and support conditions. All of these parameters mentioned in the equation are represented as a constant C. Therefore:

$$EI = \frac{1}{\delta_{exp}} C \tag{15}$$

Using Eq. (15) then the experimental values of beam flexural stiffness under fire exposure for the N and the SW can be obtained and presented in Fig. 10. In general, Fig. 10 illustrates the significant difference between the N and the SW in terms of their flexural stiffness, where the SW is far more rigid than the N. For N, it can be said that from the beginning of fire given until the temperature of 690 °C which is corresponding with a firing time of 15 minutes, the rigidity EI/C value is 0.2.

At this time, the flexural stiffness relative of SW is 5 which gives a ratio of SW to N of 25. In more detail, the comparison between the two beams is described and presented in Table III. An average ratio of 27 in the first 45 minutes of firing time and an average ratio of 19 until the firing time of 90 minutes are produced. At the last 30 minutes of the firing time (from 105 to 120 minutes) the average ratio of the flexural stiffness decreases to be 3.5.

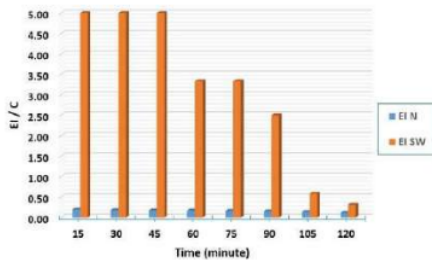


Fig. 10. Flexural stiffness variations of N and SW

TABLE III  
COMPARISON OF EI VALUES

Temperature °C	EI Relative		Ratio	Average
	N	SW		
(1)	(2)	(3)	(4)=(3)/(2)	(5)
690.03	0.200	5.000	25	
814.47	0.182	5.000	27	27
874.00	0.175	5.000	28	
917.37	0.172	3.333	19	
957.53	0.161	3.333	21	19
988.20	0.152	2.500	17	
1010.57	0.139	0.588	4	
1026.53	0.114	0.313	3	3.5

This indicates that the effective cross-section of the sandwich beam produces a moment of inertia much greater than the one of the normal concrete beam cross-section. This supports the theory of sandwich beam cross-section calculations using transformation cross-section analysis to be valid. The flexural stiffness of the N decreases dramatically following the trend in Fig. 11.

Initially, the flexural stiffness decreases significantly from the room temperature of 39.4 °C to 690 °C which corresponds to 0 to 15 minutes respectively, then decreases gradually until 1026 °C at a firing time of 120 minutes. The linear trend is obtained and presented as an equation inside Fig. 11 which produces the value  $R^2=0.979$  which means bending stiffness has a strong relationship with the temperature. The SW flexural stiffness is relatively stable for the first 45 minutes of firing time. Then, the flexural stiffness value decreases following the declining trend as shown in Fig. 12. In this case, bi-linear trend lines are proposed, the first trend line for the temperature below 874 °C the value of EI/C equals 5 and the second trend line for the temperature above 874 °C follows a linear equation as given inside Fig. 12 which produces  $R^2 = 0.882$ . This has suggested that the flexural stiffness of the beam strongly affected by the temperature and firing time.

VI.4. Deflection versus Accumulative Temperatures

Since there are three variables recorded in a single measurement in the form of deflection, time and temperature, therefore, in order to facilitate the discussion, it is necessary to simplify the presentation in the graphical form of these variables. For this reason, the time and the temperature variables are made into one parameter called accumulative temperature in a unit of °C minute. The accumulative temperature (AT) is described as a temperature cumulative over a period of time. In this case, it is considered a time period of 15 minutes. Fig. 13 demonstrates the associated graph of the deflection (in negative sign) versus the accumulative temperature for the two beams representing measurement at the surface of the beam. The deflection has been measured in the middle of the beam span. The load has been fixed so that the addition of deflection that occurs is considered the effect of firing.

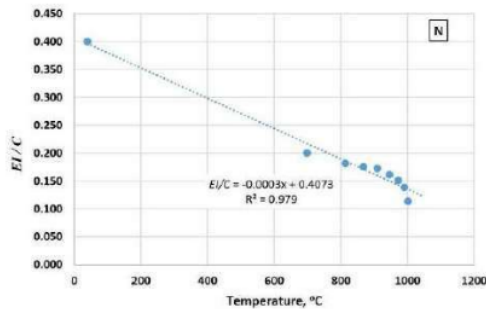


Fig. 11. The flexural stiffness of N against temperature

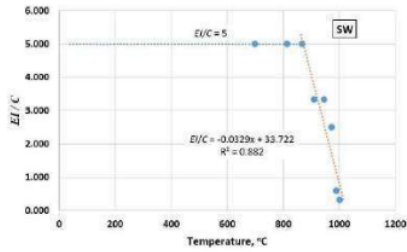


Fig. 12. The flexural stiffness of SW against temperature

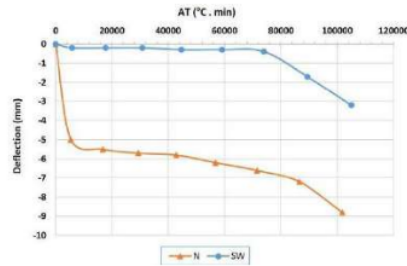


Fig. 13. Deflection against accumulative temperature

Referring to Fig. 13, the two beams have similar behaviors in terms of accumulative temperature experienced. However, the deflection experienced during the firing is significantly different. The N beam is deflected much more than the SW beam in general. In other words, the SW beam stiffs much more than the N beam. The deflection of the SW beam is lower than 1 mm until the accumulative temperature reached 75000 °C min, in contrast with the N beam where the deflection value bigger than 5 mm achieved since the accumulative temperature of 5000 °C min. It is easier to say that after the accumulative temperature of 80000 °C min, the deflection of the N beam is almost 7 times the SW beam. Before the accumulative temperature of 80000 °C min, the deflection of the N beam is more than 20 times the SW beam. The deflection of 3 mm and 8.8 mm has been obtained for the N beam and the SW beam respectively at the accumulative temperature reaches the value of about 100000 °C min.

### VI.5. Analysis of $E_c$ and $f'_c$

Since the amount of load given in this experiment for both N and SW beams has been fixed of 8.63 kN which produces a moment,  $M = M_{d,s}$  of 5.40 kNm. While based on the Eq. (9),  $M_{cr}$  for the N and the SW were obtained of 6,975 kNm and 7.97 kNm respectively. Thus, for both beams  $M_d/M_{cr} < 1$ , this means that the beams are still uncracked, so the effective moment of inertia of the beams is equal to the gross moment of inertia,  $I_g$ .

Therefore, the value of  $E_c$  can be evaluated using Eq. (16) below:

$$E_c = \frac{M}{48\delta_{exp} I_g} (3L^2 - 4a^2) \quad (16)$$

Parameters that are directly involved in the Eq. (16) are tabulated in Table IV for N and SW, then resolved for  $E_c$ . If the value of  $E_c$  is associated with  $f'_c$  according to Eq. (7) then  $f'_c$  can be approached using Eq. (17) below:

$$f'_c = \left( \frac{E_c}{4700} \right)^2 \quad (17)$$

Whereas coefficient  $E_c$  for sandwich concrete is taken from the average value of  $E_c$  of the normal concrete (100%) and the coefficient value of  $E_c$  of the lightweight concrete (75%) as described in the previous section, giving the value of 87.5% or a coefficient of 0.875. Thus the  $f'_c$  for sandwich beam can be approached using Eq. (18):

$$f'_c = \left( \frac{E_c}{0.875 \times 4700} \right)^2 \quad (18)$$

Both the  $E_c$  and the  $f'_c$  values are plotted against firing time as Fig. 14 and Fig. 15 for N and SW respectively. It is clear from the figures that the  $E_c$  and the  $f'_c$  value for the N drop significantly after the firing time in the first 15 minutes even beam strength totally lost and decreased linearly for 15 minutes incremental time of firing.

However, this is not the case with the SW where the value of the  $E_c$  and the  $f'_c$  decrease gradually until the firing time of 45 minutes and then drops gradually. At 60 minutes of the firing time, the beam strength lost almost 50%. The decreasing trend of both the  $E_c$  and the  $f'_c$  follows the naturalist logarithm function as given inside Fig. 15 with  $R^2 = 0.92$ . In short, Figures 14 and 15 demonstrate that the firing time has a significant effect on the compressive strength and modulus of elasticity of the material.

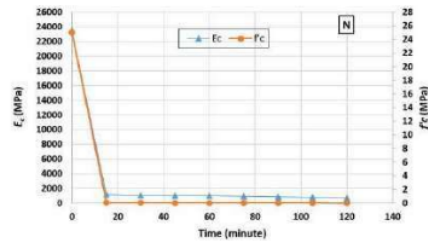


Fig. 14. Variation of  $E_c$  and  $f'_c$  against firing time of N

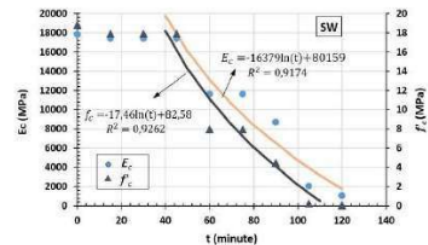


Fig. 15. Variation of  $E_c$  and  $f'_c$  against firing time of SW



TABLE IV  
 $E_c$  ANALYSIS OF N

Time (minute)	Load (kN) $M_s$ (kN m)		$3L^2 - 4a^2$	$M_s/M_{sc}$		Deflection (mm)		$I_e = I_g$ (mm <sup>4</sup> )		$E_c$ (MPa)	
				N	SW	N	SW	N	SW	N	SW
0	8,63	5,40	23000000	0,77	0,68	0,00	0,00	4,5E+08	7,43E+08	23.500,00	17.855,48
15	8,63	5,40	23000000	0,77	0,68	5,00	0,20	4,5E+08	7,43E+08	1.150,00	17.418,18
30	8,63	5,40	23000000	0,77	0,68	5,50	0,20	4,5E+08	7,43E+08	1.045,45	17.418,18
45	8,63	5,40	23000000	0,77	0,68	5,70	0,20	4,5E+08	7,43E+08	1.008,77	17.418,18
60	8,63	5,40	23000000	0,77	0,68	5,80	0,30	4,5E+08	7,43E+08	991,38	11.612,12
75	8,63	5,40	23000000	0,77	0,68	6,20	0,30	4,5E+08	7,43E+08	927,42	11.612,12
90	8,63	5,40	23000000	0,77	0,68	6,60	0,40	4,5E+08	7,43E+08	871,21	8.709,09
105	8,63	5,40	23000000	0,77	0,68	7,20	1,70	4,5E+08	7,43E+08	798,61	2.049,20
120	8,63	5,40	23000000	0,77	0,68	8,80	3,20	4,5E+08	7,43E+08	653,41	1.088,64

## VII. Conclusion

This study has shown that the temperature on the surface of the concrete beam primarily relies on firing time. The surface temperature of both beam types was similar and met standard fire. Whilst reinforcement embedded in the concrete beam experience lower temperature compares to the temperature at the beam surface where the maximum temperature of the reinforcement reached at 120 minutes of firing time is under the maximum allowable temperature of 93 °C.

The SW beam is stiffer than the N beam. The flexural stiffness of the beam has been strongly affected by the temperature and firing time. The average deflection ratio of the N beam to the SW beam is about 20 at an accumulative temperature below 80000 °C min. When the accumulative temperature at 80000 °C min the average ratio is 1. The concrete modulus of elasticity and compressive strength of the N beam decrease significantly after 15 minutes the firing time and the beam strength was totally lost. The SW beam strength decreases slightly until the firing time of 45 minutes and then drops gradually. The beam strength has been lost almost 50% at 60 minutes of firing time.

## Acknowledgements

The authors acknowledge the financial support for this research from the Indonesian Ministry of Research, Technology and Higher Education through the Fundamental Research Scheme.

## References

- [1] Chythanya, M. (2009). *Finite Element Analysis on the Effect of Fire for Specified Duration on a Reinforced Concrete Beam with Varied Boundary Conditions*, Florida State University
- [2] Choi, E. G.; Shin, Y. S. (2011), The structural behavior and simplified thermal analysis of normal-strength and high-strength concrete beams under fire, *Engineering Structures*, Vol. 33, No. 4, 1123–1132. doi:10.1016/j.engstruct.2010.12.030
- [3] Kodur, V. K. R.; Agrawal, A. (2017), Effect of temperature induced bond degradation on fire response of reinforced concrete beams, *Engineering Structures*, Vol. 142, No. 2017, 98–109. doi:10.1016/j.engstruct.2017.03.022
- [4] Wang, Y.; Yuan, G.; Huang, Z.; Lyu, J.; Li, Q.; Long, B. (2018). Modelling of reinforced concrete slabs in fire, *Fire Safety Journal*, Vol. 100, No. September, 171–185. doi:10.1016/j.firesaf.2018.08.005
- [5] Venkatesh, K. (2014). Properties of Concrete at Elevated Temperatures, *ISRN Civil Engineering*, Vol. 2014, No. March, 1–15. doi:10.1155/2014/468510
- [6] Jiang, C. J.; Yu, J. T.; Li, L. Z.; Wang, X.; Wang, L.; Liao, J. H. (2018), Experimental study on the residual shear capacity of fire-damaged reinforced concrete frame beams and cantilevers, *Fire Safety Journal*, Vol. 100, No. September, 140–156. doi: 10.1016/j.firesaf.2018.08.004
- [7] Jocius, V., Skripkiūnas, G., Lipinskas, D., Effect of Aggregate on the Fire Resistance of Concrete, (2014) *International Review of Civil Engineering (IRECE)*, 5 (4), pp. 118–123. doi: https://doi.org/10.15866/irece.v5i4.2165
- [8] Benoudjafer, I., Labbaci, B., Benoudjafer, I., Effect of Local Temperature During Service on the Mechanical Properties of Concrete, (2016) *International Review of Civil Engineering (IRECE)*, 7 (3), pp. 57–62. doi: https://doi.org/10.15866/irece.v7i3.8851
- [9] Miloudi, M., Merbouh, M., Glaoui, B., Mechanical Properties of Concrete Using Coal Waste (Heap) as Partial Replacements of Fine Aggregate in Hot Weather, (2017) *International Review of Civil Engineering (IRECE)*, 8 (4), pp. 120–124. doi: https://doi.org/10.15866/irece.v8i4.12273
- [10] Ahmed, S., Salih, M., Durability of Concrete Containing Different Levels of Supplementary Cementitious Materials, (2018) *International Review of Civil Engineering (IRECE)*, 9 (6), pp. 241–247. doi: https://doi.org/10.15866/irece.v9i6.15859
- [11] Turkowski, P.; Lukomski, M.; Sulik, P.; Roszkowski, P. (2017). Fire Resistance of CFRP-strengthened Reinforced Concrete Beams under Various Load Levels, *Procedia Engineering*, Vol. 172, No. 2017, 1176–1183. doi:10.1016/j.proeng.2017.02.137
- [12] Carlos, T. B.; Rodrigues, J. P. C.; de Lima, R. C. A.; Dhima, D. (2018). Experimental analysis on flexural behaviour of RC beams strengthened with CFRP laminates and under fire conditions, *Composite Structures*, Vol. 189, No. April, 516–528. doi:10.1016/j.compstruct.2018.01.094
- [13] Truong, G. T.; Lee, H. H.; Choi, K. K. (2018). Flexural behavior of RC beams strengthened with NSM GFRP strips after exposed to high temperatures, *Engineering Structures*, Vol. 173, No. Oktober, 203–215. doi:10.1016/j.engstruct.2018.06.110
- [14] Jin, L.; Zhang, R.; Dou, G.; Du, X. (2018). Fire resistance of steel fiber reinforced concrete beams after low-velocity impact loading, *Fire Safety Journal*, Vol. 98, No. April, 24–37. doi: 10.1016/j.firesaf.2018.04.003
- [15] Akmaluddin; Murtiadi, S.; Gazalba, Z. (2016). Structural Behavior of Steel Reinforced Sandwich Concrete Beam with Pumice Lightweight Concrete Core, *Applied Mechanics and Materials*, Vol. 845, 158–165. doi: 10.4028/www.scientific.net/AMM.845.158
- [16] Keskes, B., Abbadi, A., Azari, Z., Bouaouadja, N., Static and Fatigue Characterization of Nomex Honeycomb Sandwich Panels, (2015) *International Review of Civil Engineering (IRECE)*, 6 (4), pp. 81–87. doi: https://doi.org/10.15866/irece.v6i4.7971
- [17] Kabay, N.; Tufekci, M. M.; Kizilkanat, A. B.; Oktay, D. (2015). Properties of concrete with pumice powder and fly ash as cement

replacement materials, *Construction and Building Materials*, Vol. 85, 1–8.

doi:10.1016/j.conbuildmat.2015.03.026

- [18] Muralitharan, R. S.; Ramasamy, V. (2015). Basic Properties of Pumice Aggregate, *International Journal of Earth Sciences and Engineering*, Vol. 08, No. 04, 256–263
- [19] SNI-1741:2008. (2008). *How to Test Building Materials for Fire Danger Prevention in Building Buildings and Buildings*, BSNi
- [20] Akmaluddin, A. (2011). Effect of Tensile Reinforcement Ratio on the Effective Moment of Inertia of Reinforced Lightweight Concrete Beams for Short Term Deflection Calculation, *ITB Journal of Engineering Science*, Vol. 43, No. 3, 209–226.  
doi: 10.5614/itbj.eng.sci.2011.43.3.4
- [21] Kodur, V. K. R.; Hamathy, T. Z. (2016). *Properties of Building Materials, SFPE Handbook of Fire Protection Engineering*, Fifth Edition.  
doi: 10.1007/978-1-4939-2565-0\_9
- [22] Murad, Y., Abu Zaid, J., Finite Element Modelling of Reinforced Concrete Beams Strengthened with Different Configuration of Carbon Fiber Sheets, (2019) *International Review of Civil Engineering (IRECE)*, 10 (4), pp. 188-196.  
doi: <https://doi.org/10.15866/irece.v10i4.16870>
- [23] Sapountzakis, E., An Improved Model for the Analysis of Plates Stiffened by Parallel Beams Including Creep and Shrinkage Effects: Application to Concrete or to Composite Steel-Concrete Structures, (2018) *International Journal on Engineering Applications (IREA)*, 6 (2), pp. 57-70.  
doi: <https://doi.org/10.15866/irea.v6i2.15377>

## Authors' information

Civil Engineering Department, Faculty of Engineering, Universitas Mataram, Jalan Majapahit No. 62, Mataram, Indonesia. 83125.



**Akmaluddin Akmaluddin** was born in Indonesia. Degree of B.Eng. has obtained from Universitas Mataram in 1993. The MSc.(Eng.) and Ph.D degree were obtained from the University of Liverpool in 2000 and 2004 respectively in the civil engineering field of study. He published several journal and conference papers with a research interest in the concrete structure and development of local material as well as building assessment using non-destructive testing. Dr. Akmaluddin is a member of the Indonesian construction expertise association, representative council of West Nusa Tenggara, Indonesia.

# Flexural Stiffness of Normal and Sandwich Reinforced Concrete Beam Exposed to Fire Under Fixed Loading

ORIGINALITY REPORT

7%

SIMILARITY INDEX

9%

INTERNET SOURCES

0%

PUBLICATIONS

3%

STUDENT PAPERS

PRIMARY SOURCES

1

[www.scilit.net](http://www.scilit.net)

Internet Source

7%

Exclude quotes On

Exclude matches < 3%

Exclude bibliography On